The μ-RWELL detector for high particle rate

G. Bencivenni, G. Felici, M. Gatta, M. Giovannetti,
G. Morello, M. Poli Lener

and on behalf of LHCb Collaboration
Laboratori Nazionali di Frascati - INFN

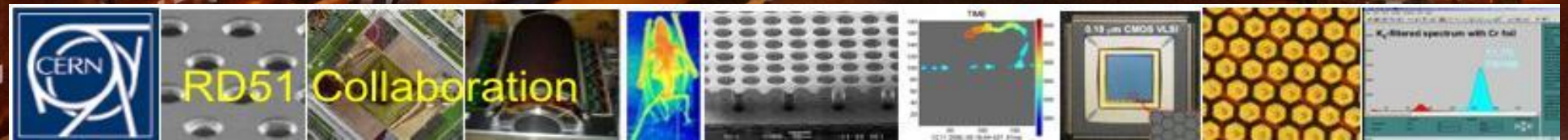

OUTLINE

- Detector architecture & principle of operation
- The single-resistive layout
- High rate layouts: design & performance at PSI
- High space resolution
- Summary

LHCb UPGRADE

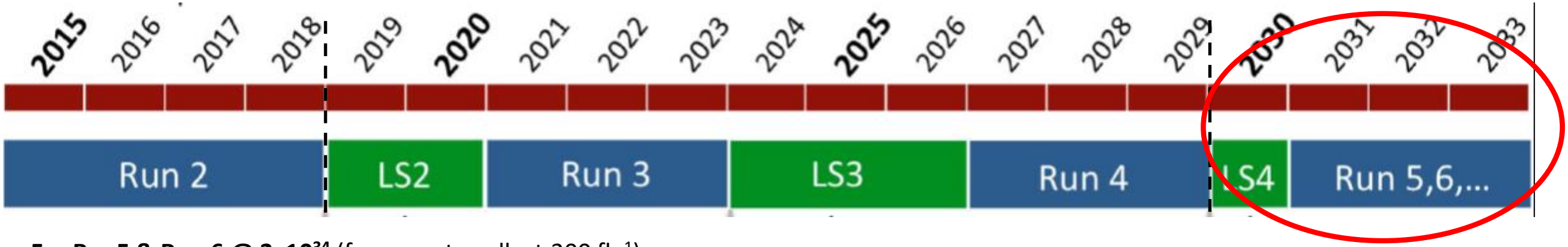

For Run5 & Run 6 @ 2x10^{34} (foreseen to collect 300 fb^{-1}):

Estimated fluxes for phase II Muon Apparatus

	kHz/cm^2		kHz/cm^2		kHz/cm^2		kHz/cm^2
M2R1	3300	M3R1	1900	M4R1	650	M5R1	550
M2R2	300	M3R2	220	M4R2	85	M5R2	55
M2R3	35	M3R3	19	M4R3	9	M5R3	7
M2R4	20	M3R4	5	M4R4	3	M5R4	4

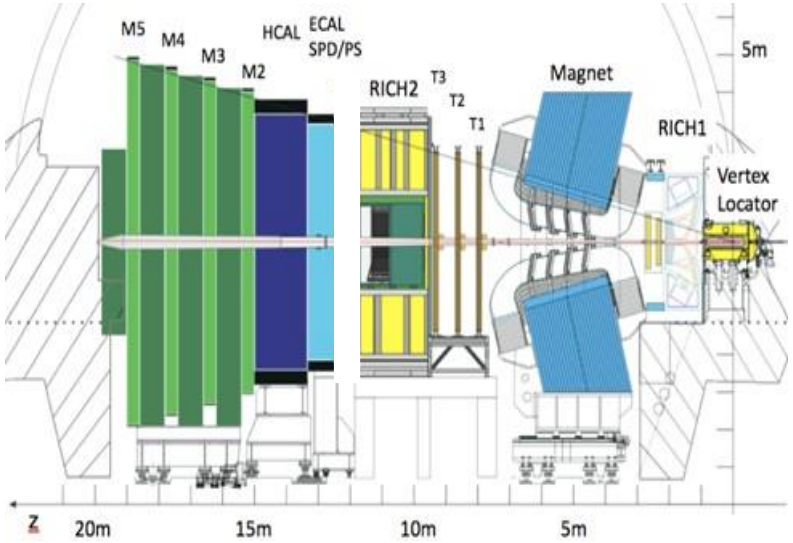

μ-RWELL for LHCb MUON Upgrade

M2 station - max rate (kHz/cm^2)

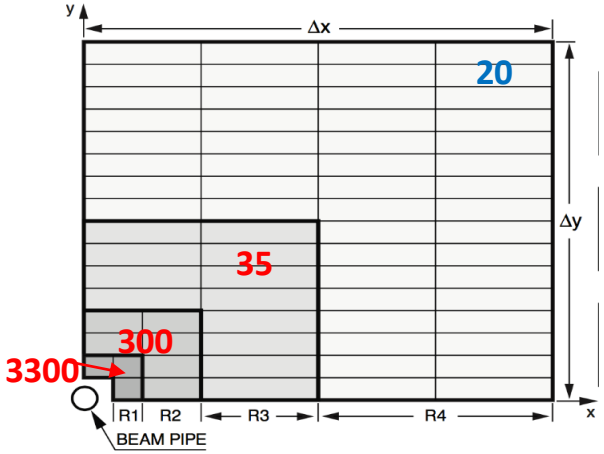

Detector requirements:

- **Rate up to 3 MHz/cm2 on detector**
- **Rate up to 1 MHz on FEE channel**
- **Efficiency > 97%** within a BX (25 ns)
- **Long stability** up to **6 C/cm2** acc. charge in **10 y** of operation (M2R1)
- **Pad cluster size < 1.2**

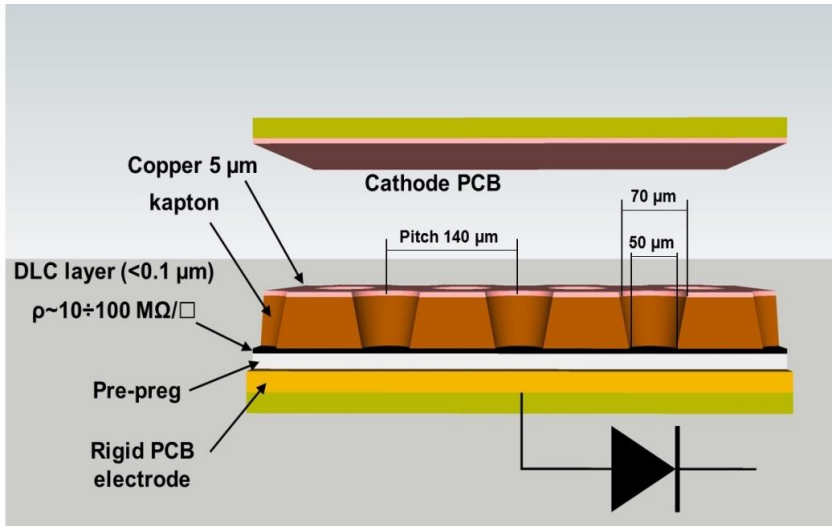

G. Bencivenni et al., 2015_JINST_10_P02008

The μ-RWELL is composed of only two elements: the μ-RWELL_PCB and the cathode

The μ-RWELL_PCB, the core of the detector, is realized by coupling:

1. **a WELL patterned Apical® foil acting as amplification stage**
2. **a resistive layer for discharge suppression w/surface resistivity ~ 10 ÷ 100 MΩ/□ - with different current evacuation schemes:**
   i. **Low Rate scheme << 1 MHz/cm^2 - SHiP, CepC, STCF, EIC, HIEPA**
   ii. **High Rate scheme >>1 MHz/cm^2 - LHCb-Muon upgrade & future colliders - CepC, Fcc-ee/hh**
3. **a standard readout PCB**

Principle of operation

Applying a suitable voltage between the **top Cu-layer and the DLC** the **"WELL" acts as a multiplication channel** for the ionization produced in the conversion/drift gas gap.

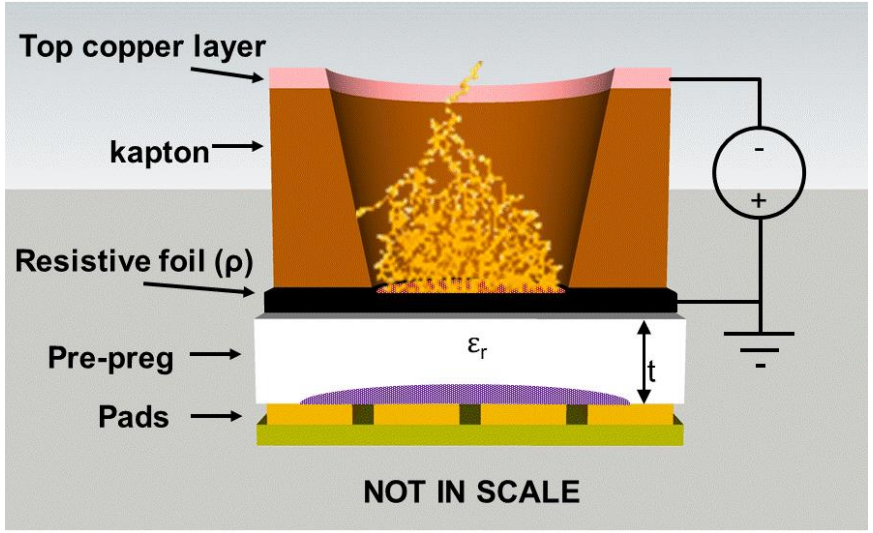

The charge induced on the resistive foil is dispersed with a *time constant,* $\tau \sim \rho \times C$ [*M.S. Dixit et al., NIMA 566 (2006) 281*]:

- the DLC surface resistivity → ρ
- the capacitance per unit area, which depends on the distance between the resistive foil and the pad/strip readout plane → t
- the dielectric constant of the insulating medium → ε_r

$$C = \varepsilon_0 \times \varepsilon_r \times \frac{S}{t}$$

- The main effect of **the introduction of the resistive stage** is the **suppression of the transition from streamer to spark**, with a consequent reduction of the spark-amplitude
- As a drawback, the **capability to stand high particle fluxes is reduced**, but **appropriate grounding schemes** of the resistive layer **solves this problem** (*see High Rate layouts*)

Detector Gain

Ar/CO2/CF4=45/14/40 & Beam spot ~ 4 cm^2

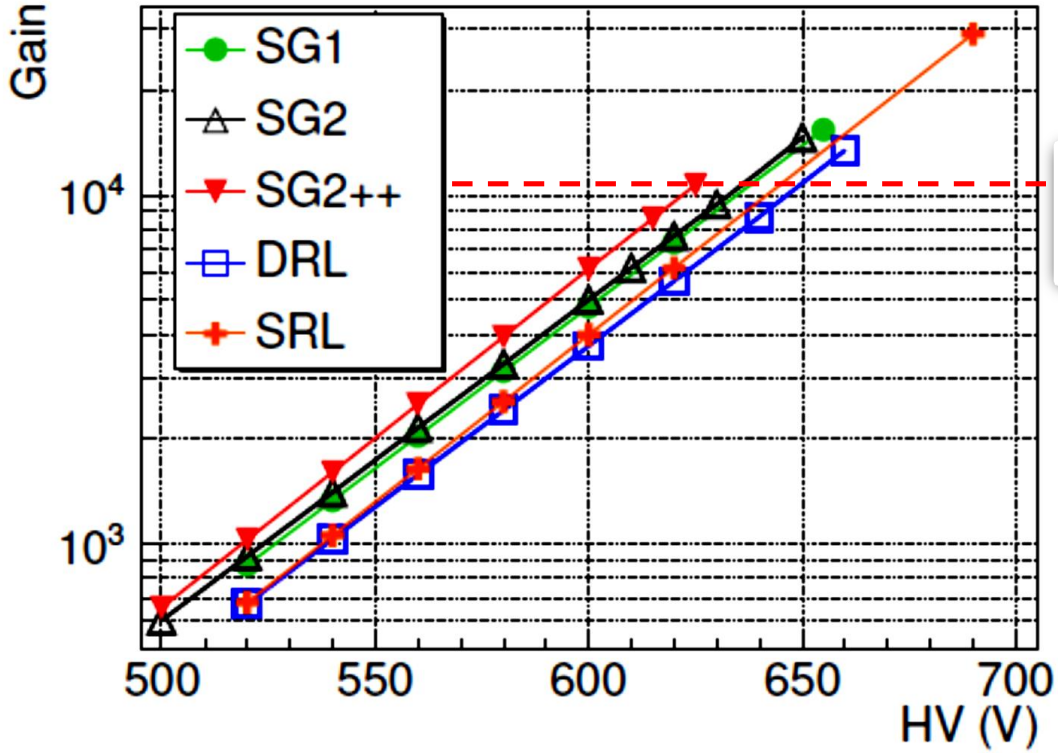

Gain up to 10^4
with single amplication stage

Gas gain of detectors as measured with a 270 MeV/c π+ beam at PSI with particle fluxes ranging from $\sim$ 320 kHz/cm^2 up to $\sim$ 1.2 MHz/cm^2.

The Low Rate Layout

Easy Technological Transfer (TT) to industry

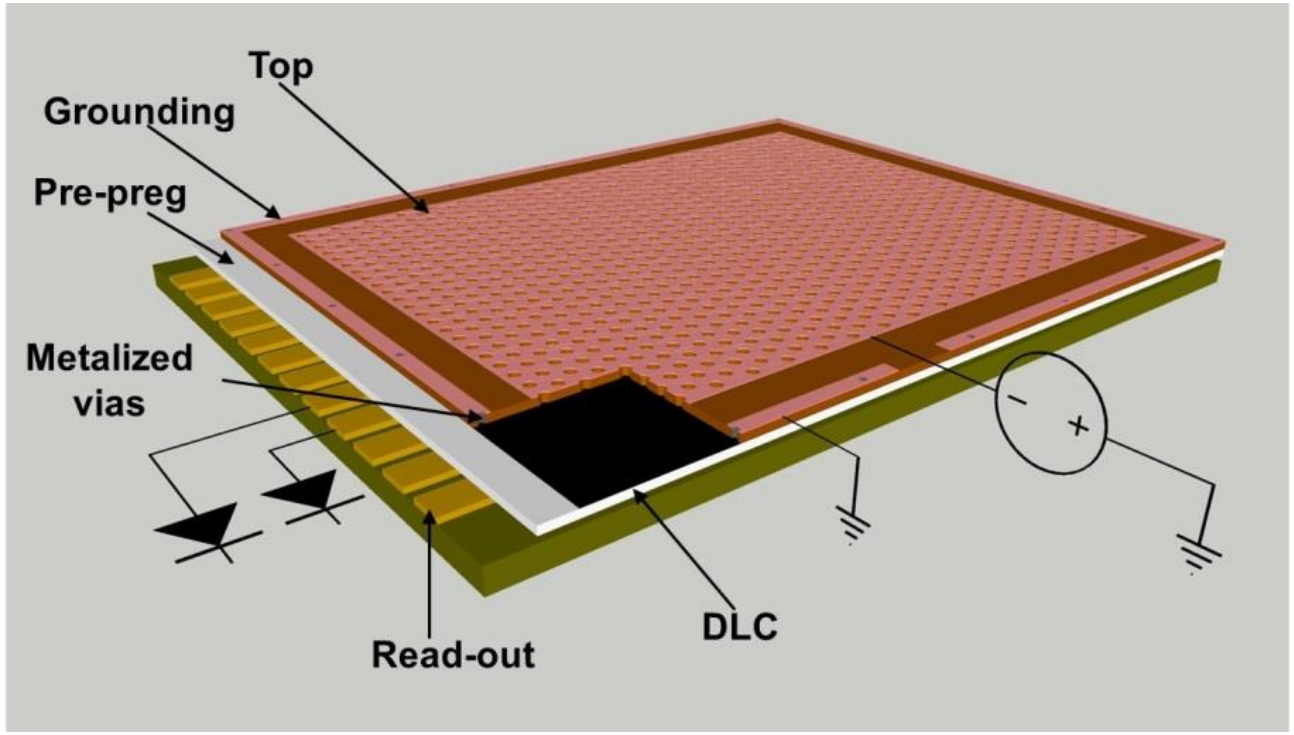

Single Resistive Layer (SRL): 2-D current evacuation scheme based on a **single resistive layer** with a conductive **grounding all around the perimeter** of the active area.

For **large area detectors** the **path of the current towards the ground connection** could be large and strongly dependent on the particle incident point giving rise to **large detector response inhomogeneity.**

High rate layouts

To overcome the intrinsic limitation of the Single Resistive layout with edge grounding **the solution is to reduce as much as possible the paths towards the ground connection** introducing a **high density "grounding network"** on the resistive stage of the detector.

Two layouts with a "dense" grounding network scheme have been designed and implemented:

- the **Double Resistive layer** (DRL) with a sort of **3-D grounding** scheme
- the **Single Resistive layout with a grounding grid** (SG) deposited on the resistive stage

HR layouts: the Double-Resistive Layer

Not Easy TT to industry

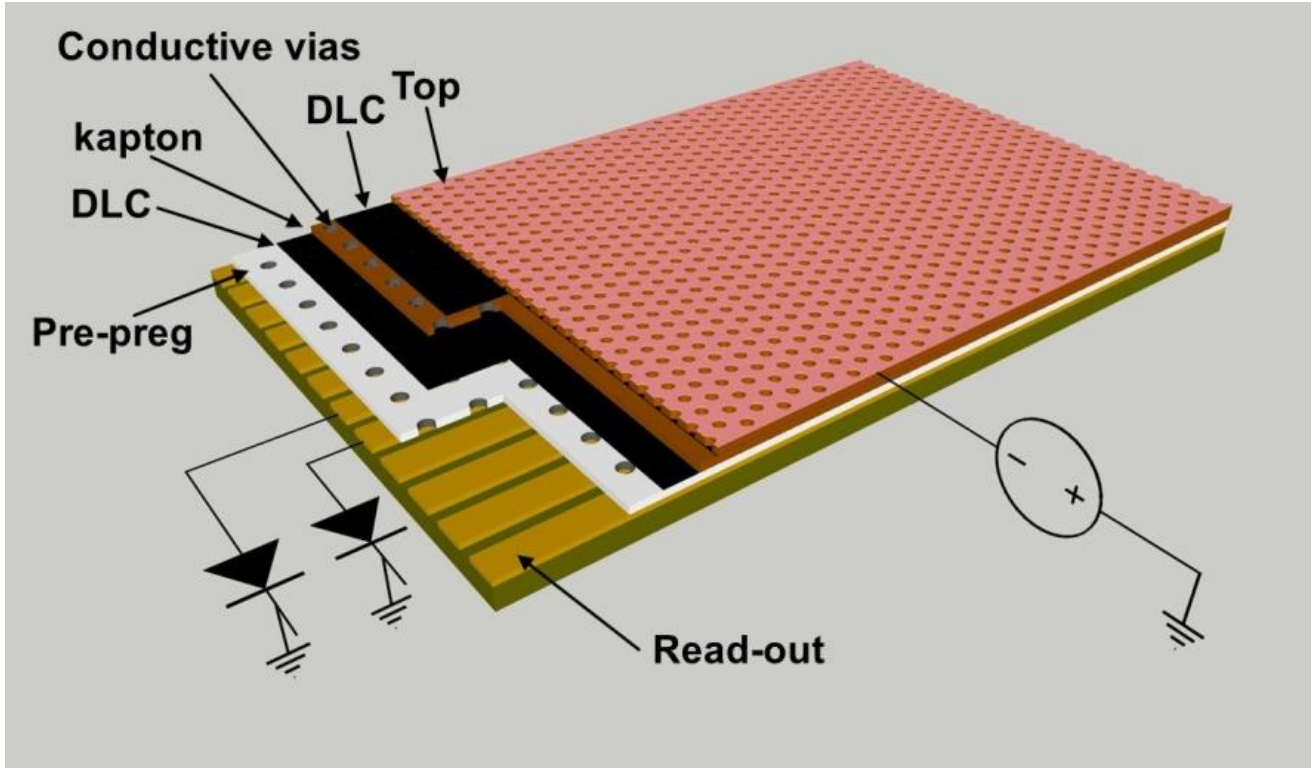

Double Resistive Layer (DRL): 3-D current evacuation scheme based on **two stacked resistive layers** connected through a **matrix of conductive vias** and **grounded through a second matrix of vias to the underlying readout** electrodes. The **pitch of the vias** can be easily done with a density **less than 1/cm^2**.

HR layouts: the Silver Grid

Easy TT as SRL scheme

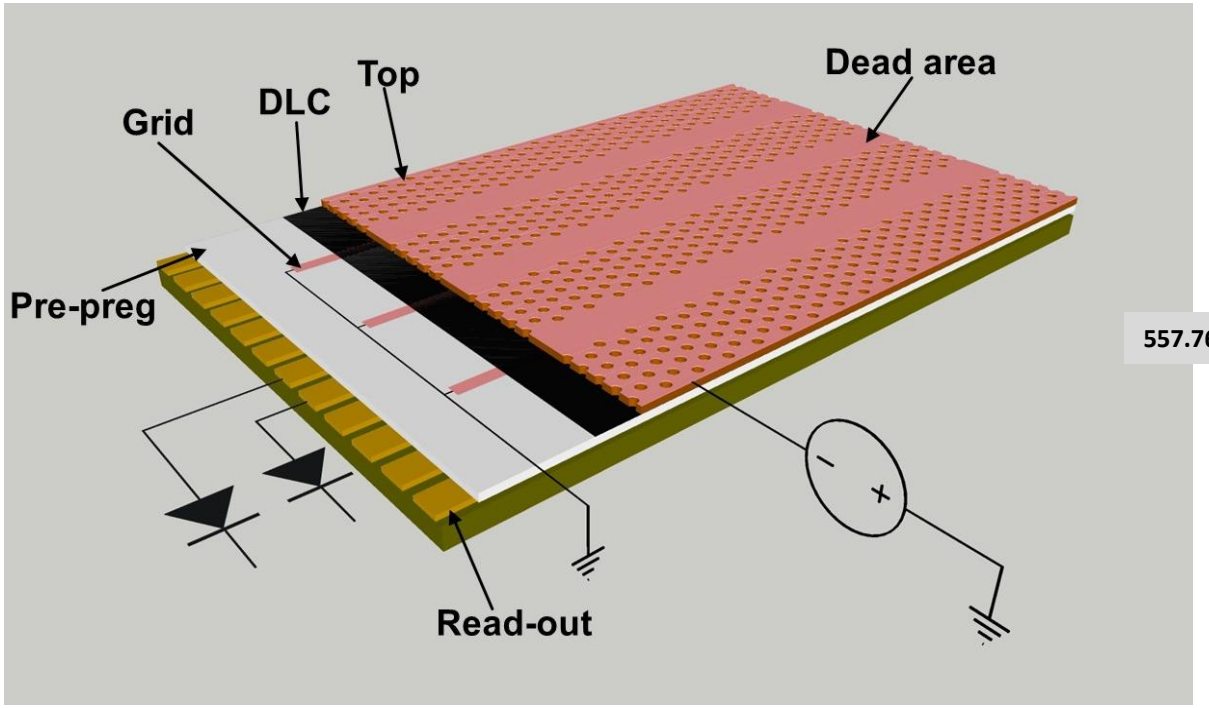

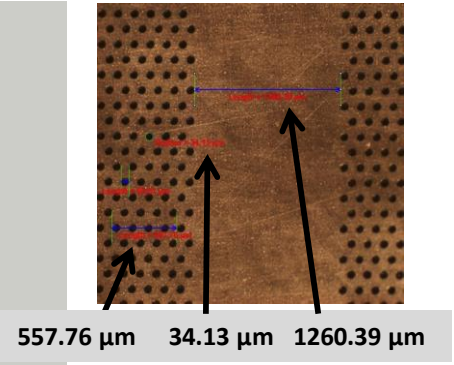

A **simplified HR scheme based on a Single Resistive layer** with the implementation of a **2-D grounding** based on **conductive strip lines** realized on the DLC layer.
The **conductive grid** can be screen-printed or better etched by photo-lithography (*if a Cu deposition is done above the DLC layer → USTC – Hefei R&D*).

The **conductive grid** can **induce instabilities due to discharges over the DLC surface**, thus requiring for the **introduction of a small dead zone** on the amplification stage

HR layouts performance: the efficiency

Ar/CO2/CF4=45/14/40 & Beam spot ~ 4 cm^2

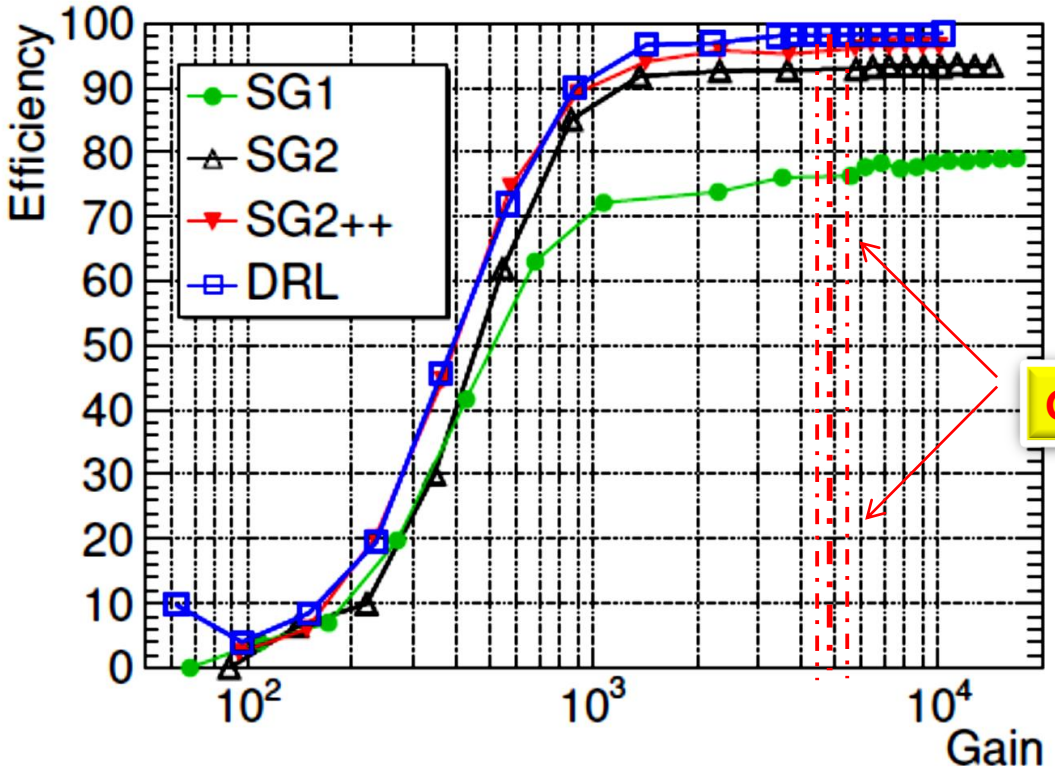

G = 5000 ± 10%

The DRL layout reaches full tracking efficiency , 98% (NO DEAD ZONE).
The SG1, SG2 and SG2++ show lower efficiency (76% - 93% - 97%) BUT higher than their geometrical acceptance (66% - 90% - 95% respectively), thanks to the efficient electron collection mechanism that reduce the effective dead zone.

Rate capability of HR Layouts

Ar/CO2/CF4=45/14/40 & G= 5000 & Beam spot ~ 4 cm^2

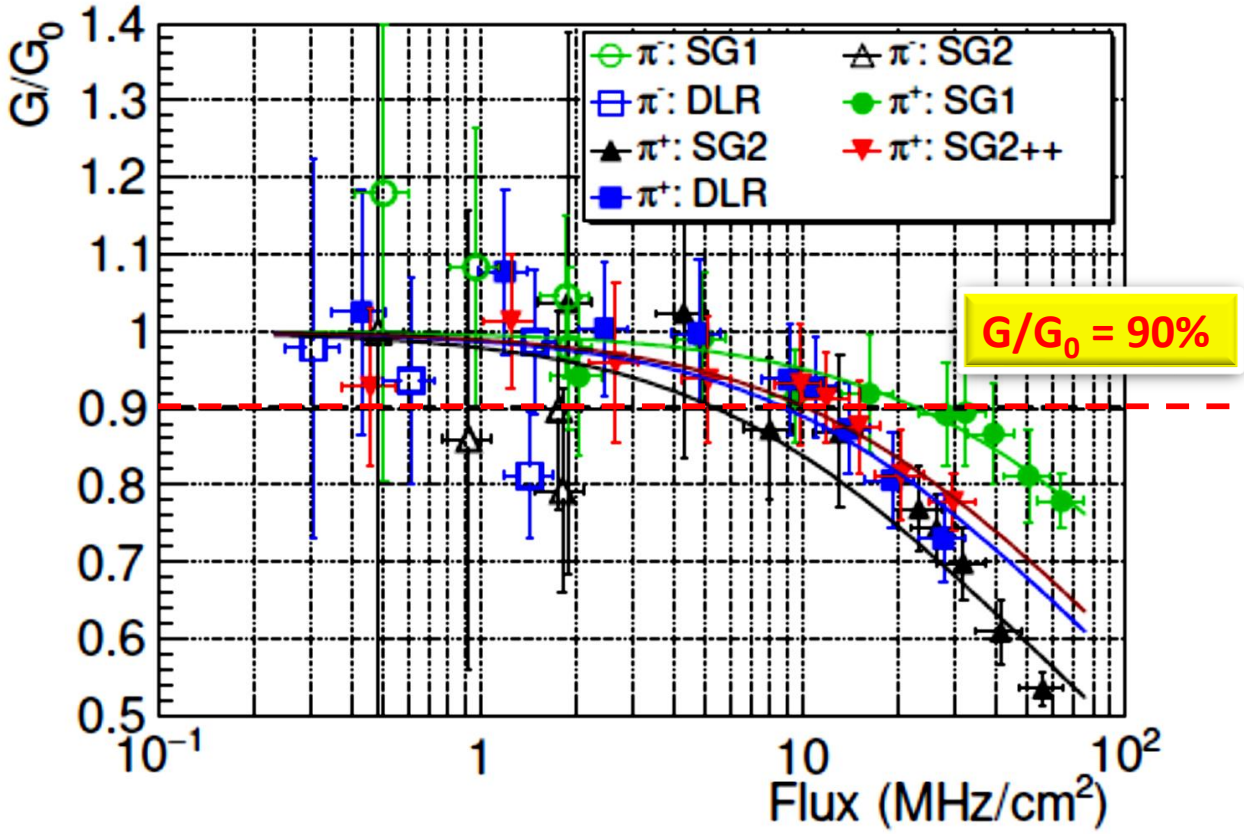

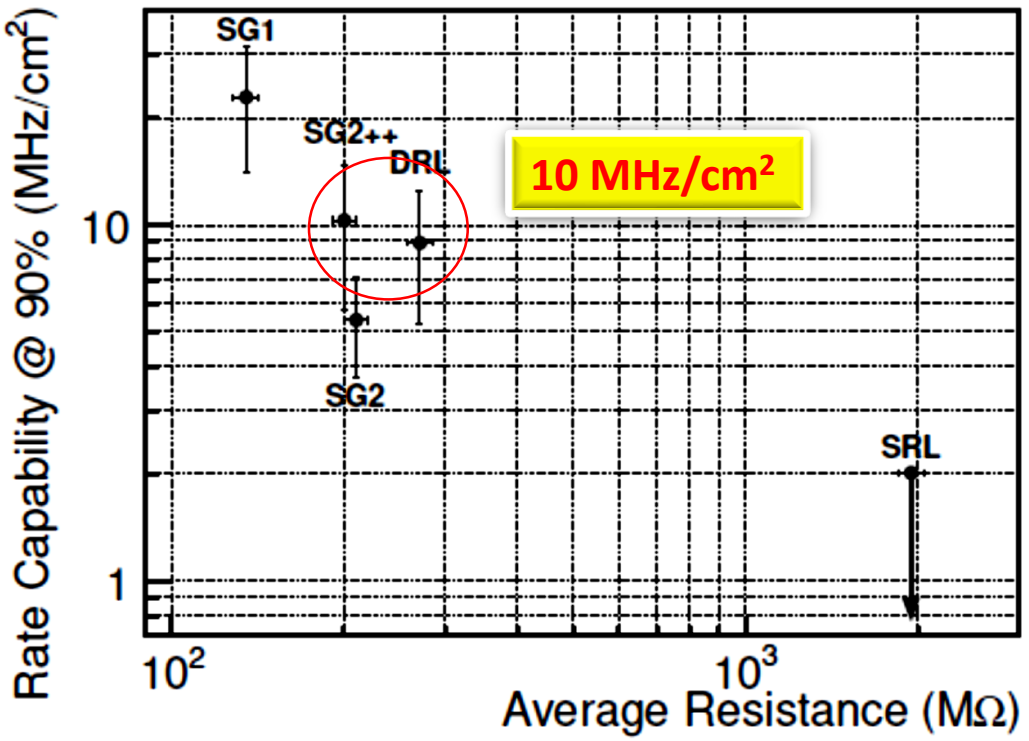

The gain drop is due to the Ohmic effect on the resistive layer: the current collected on the DLC drift towards the ground "through" an effective average resistance Ω_{eff}, depending on the evacuation scheme geometry and the DLC surface resistivity.

Time Performance

Ar/CO2/CF4=45/14/40

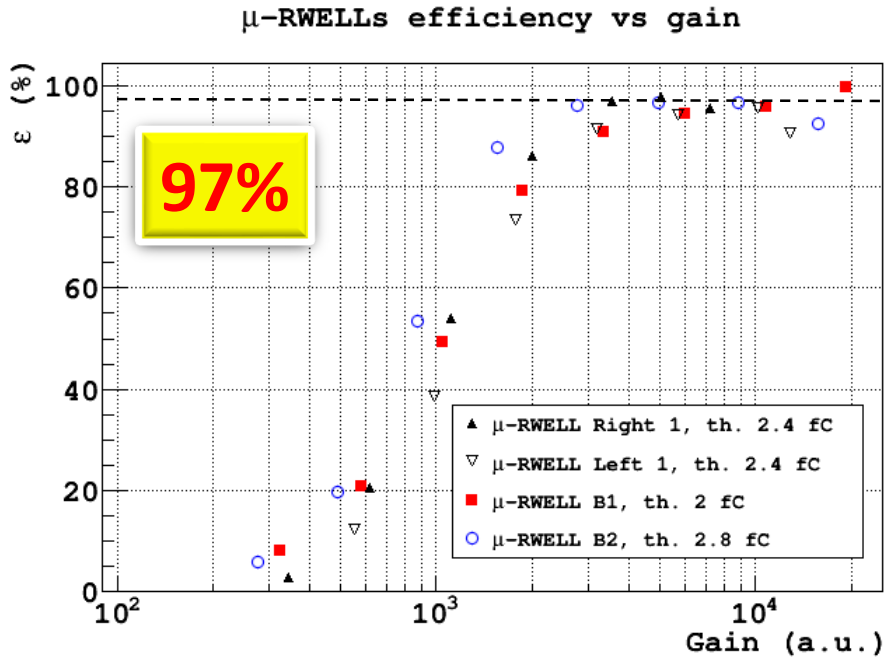

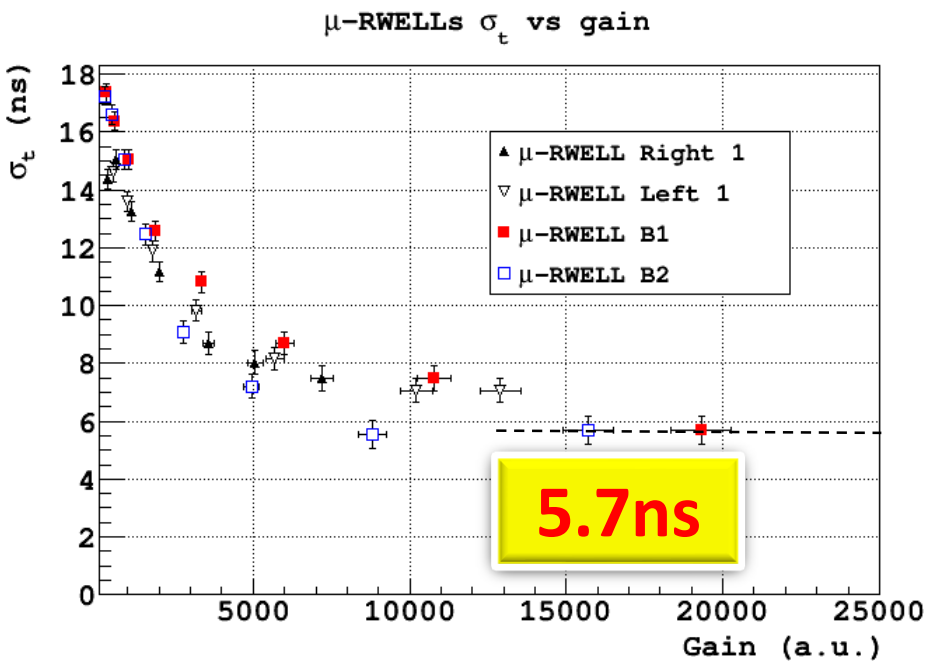

Different chambers with different dimensions and resistive schemes exhibit a very similar behavior although realized in different sites (large detector realized @ ELTOS).

The saturation at 5.7 ns is dominated by the **FEE** (measurement with VFAT2)[1]

Measurements done with **GEM by LHCb group gave σ_t = 4.5 ns with VTX chip**, constant fraction discriminator [2].

[1] G. Bencivenni et al, **"Performance of u-RWELL detector *vs* resistivity of the resistive stage", NIM A 886 (2018) 36**

[2] G. Bencivenni et al, "Performance of a triple-GEM detector for high rate charged particle triggering", NIM A 494 (2002) 156

Space resolution vs inclined tracks: μ-TPC mode

For inclined tracks and/or in presence of high B field, **the charge centroid method gives a very broad spatial distribution** on the anode-strip plane.

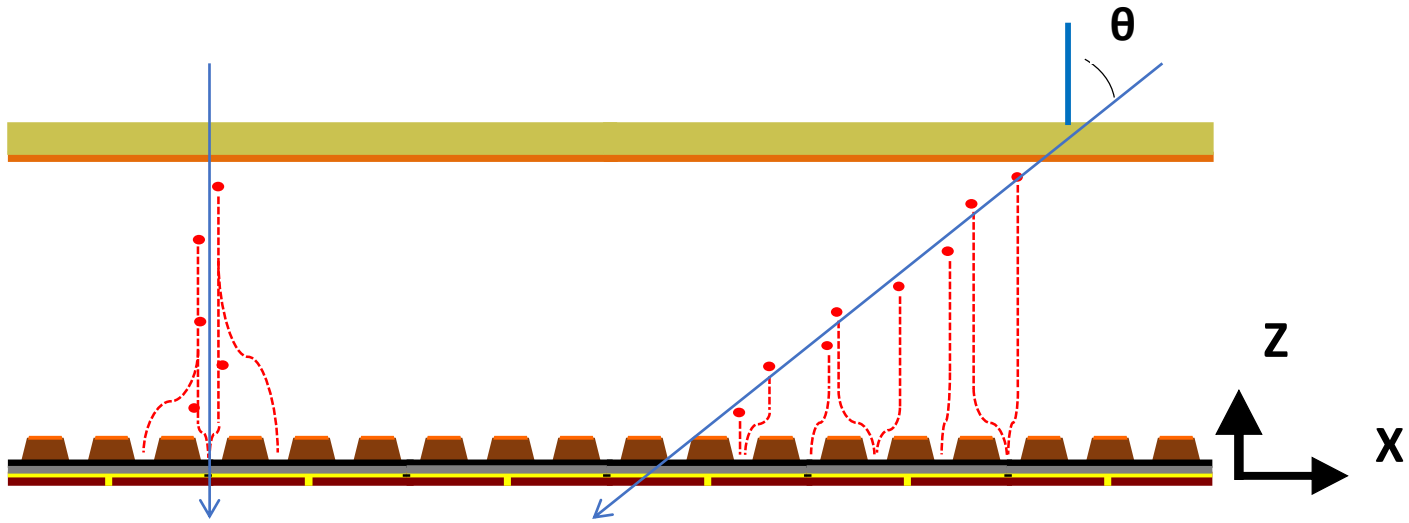

In the **u-TPC mode,** *introduced for MMs by T. Alexopoulos (NIM A 617 (2010) 161),* from **the knowledge** of the **drift time** of primary electrons, **each ionization cluster is projected inside the conversion gap**, and the track segment in the gas gap is reconstructed.

Space resolution vs inclined tracks: µ-TCP mode

Thanks to the collaboration with BESIII-CGEM, G. Cibinetto, R.Farinelli (Ferrara) & L.Lavezzi (To)

Ar:CO_2:CF_4 45:15:40 - HV=600V, Ed=1kV/cm, Gain ~10^4

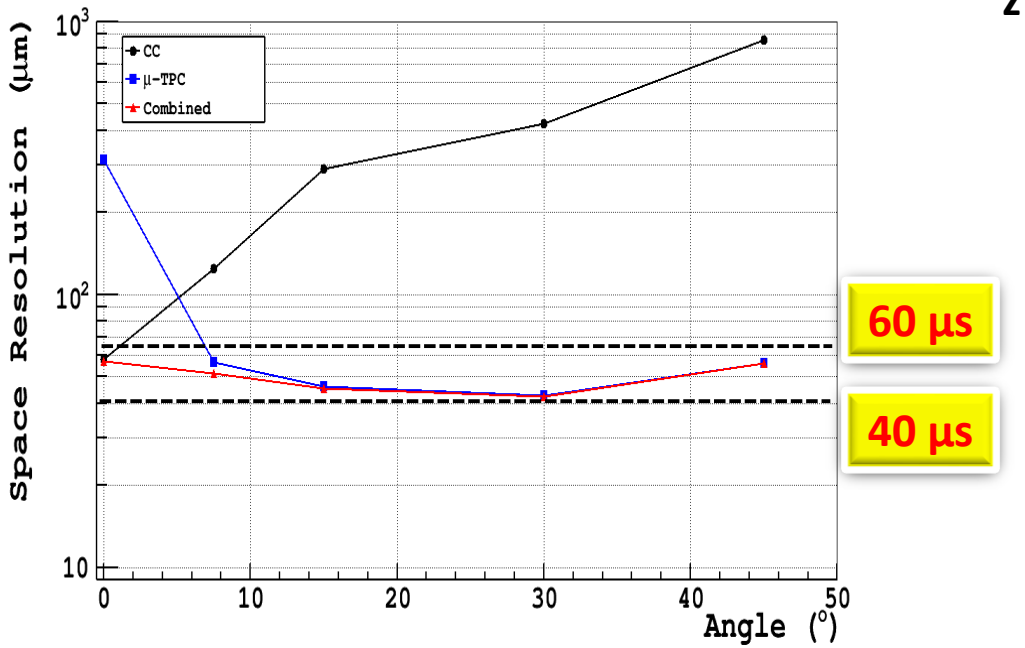

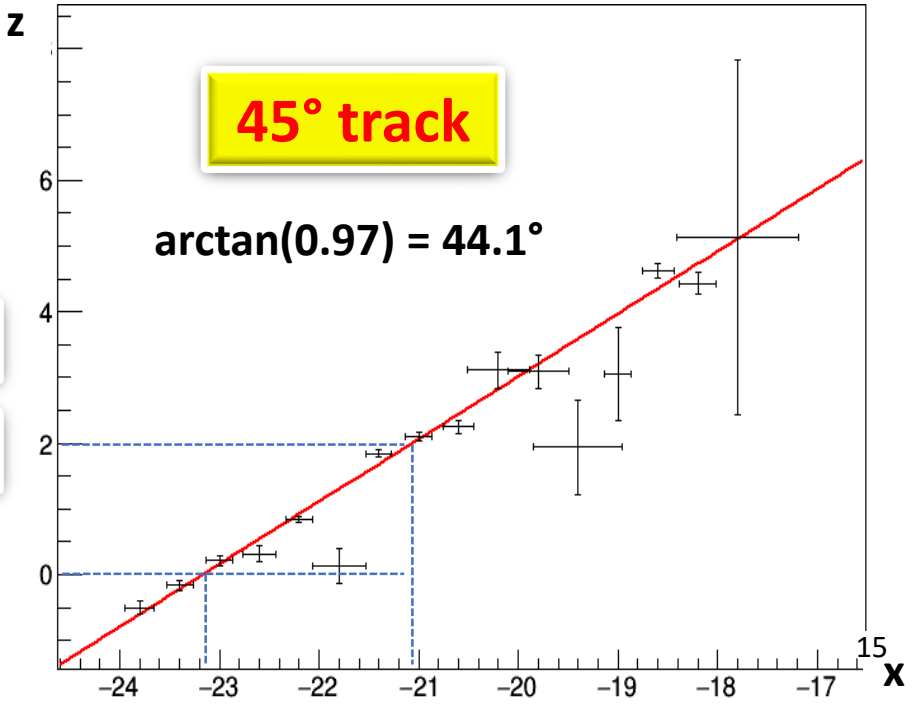

Combining the CC and the µ-TPC mode with E_d= 1 kV/cm a spatial resolution (40÷60 µm) almost flat over a wide range of incidence angles is obtained

Summary

The μ-RWELL is a single-amplification stage, spark-protected resistive MPGD based on a breakthrough technology suitable for very large area planar tracking devices.

The detector has been characterized:

- gas gain ≥ 10^4
- rate capability ~ 10 MHz/cm^2 *(w/HR layouts)*
- space resolution < 60μm *(over a large incidence angle of the tracks)*
- time resolution ~ 5.7 ns

Status of the R&D/engineering:

- Low rate (<100kHz/cm^2) :
  - small and large area prototypes built and extensively tested
  - Technology Transfer to industry (@ ELTOS) well advanced
- High rate (>1 MHz/cm^2):
  - several layouts under study showing very promising performance
  - the engineering and the TT to industry will be started in 2019
- R&D on DLC manufacturing processes, stability under irradiation and current flow is on going

Breaking News: the uRANIA proposal (μ-RWELL Advanced Neutron Imaging Apparatus) has been recently selected for funding within ATTRACT call

BACKUP

Discharge studies

The μ-RWELL discharge probability measured at the PSI, and compared with the measurement done with GEM in the same period and in the 2004 (*same gas mixture - Ar:CO_2:CF_4 = 45:15:40*).

The measurement has been done in current mode, with an intense 270 MeV/c π^+ beam, with a proton contamination of the 3.5%.

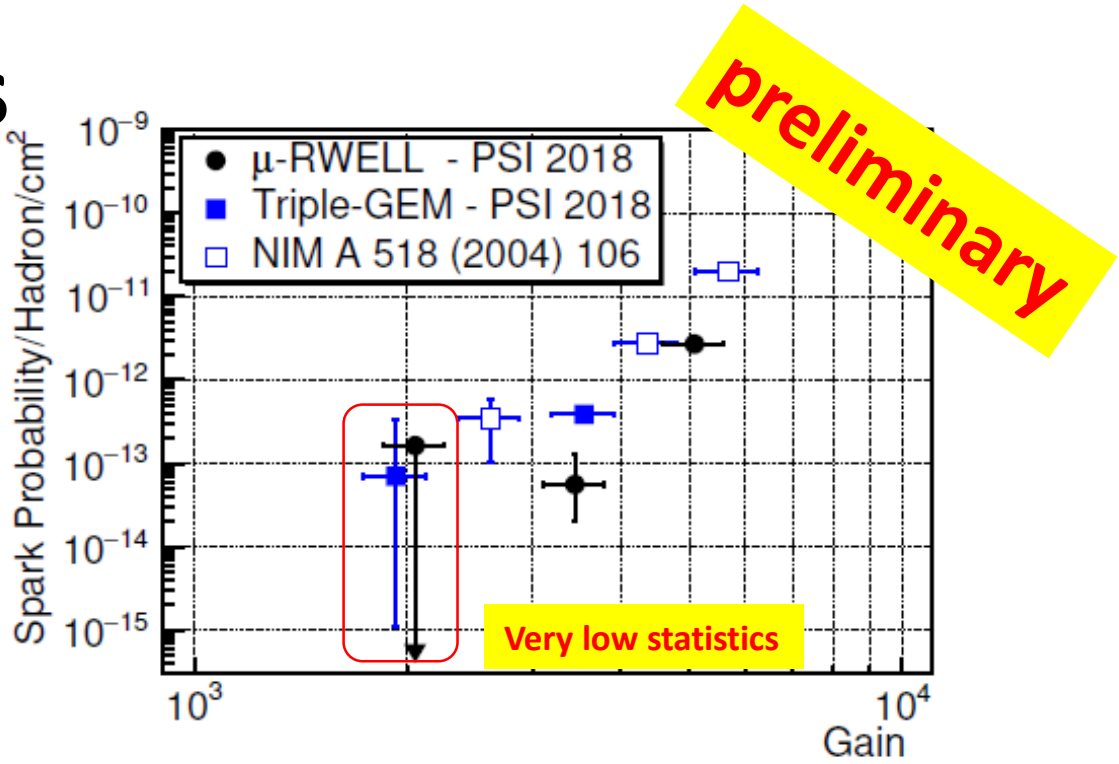

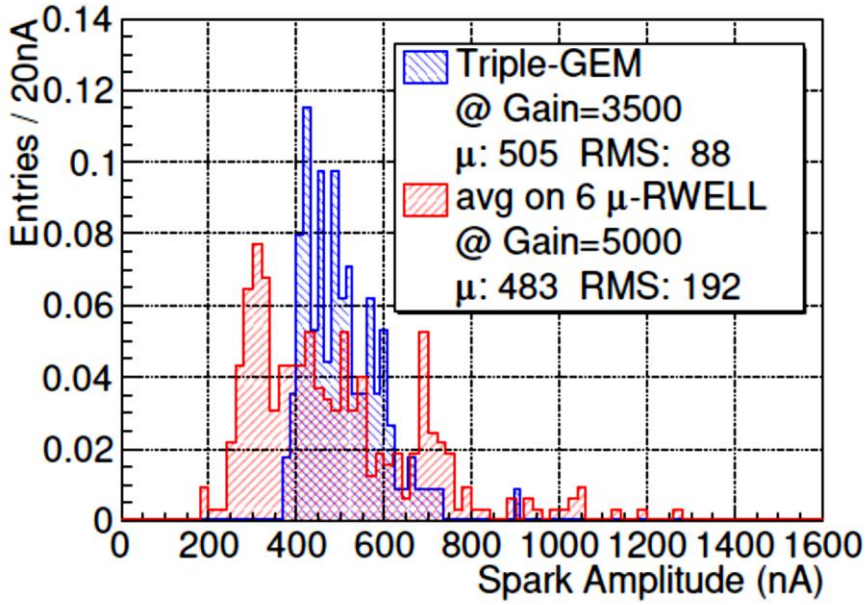

A "discharge" has been defined as the current spike exceeding the steady current level correlated to the particle flux (~90 MHz on a ~5 cm^2 beam spot size).

The discharge probability for μ-RWELL comes out to be of the same order of magnitude of the one measured for GEM.

While its discharge amplitude seems to be lower than the one measured for GEM.

VFAT3 CHIP

VFAT3 front-end chip (128 ch. &130 nm CMOS tech.) is currently under design for the readout of triple-GEM detectors of the CMS phase 1 upgrade ➔
It looks to be an useful starting point on which adjust our needs

VFAT3 features:

1. selectable peaking time

Tpeak [ns]	Delay time Td [ns]
25	15
50	29
75	43.4
100	57.8

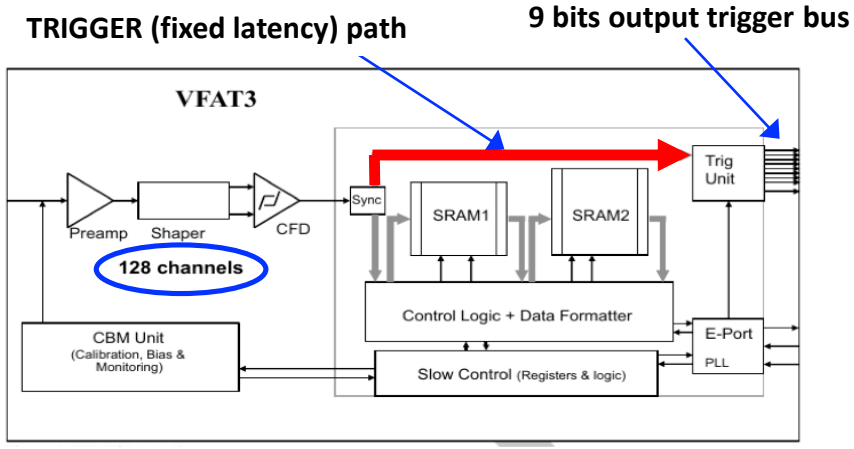

1. **rate capability = 1 MHz @ T_{PEAK} = 25 ns**
2. time resolution ~ 6 ns @ T_{PEAK} = 25 ns
3. noise $e_{RMS} \leq$ 1000e @ T_{PEAK}= 25 ns, pad capacitance < 100 pF
4. to transfer 128 channels (bits) in 25 ns ➔ 8 bits bus + 640 MHz clock (40 MHz × 16)

G. Felici (LNF), F. Loddo (Bari)

Technology Transfer to Industry

The **engineering and industrialization** of the μ-RWELL technology is one of the main objective of the project.

Production Tests @ ELTOS (http://www.eltos.it)
small detectors:

- 10x10 cm^2 PCB – (PAD r/o)
- 10x10 cm^2 PCB – (strip r/o)

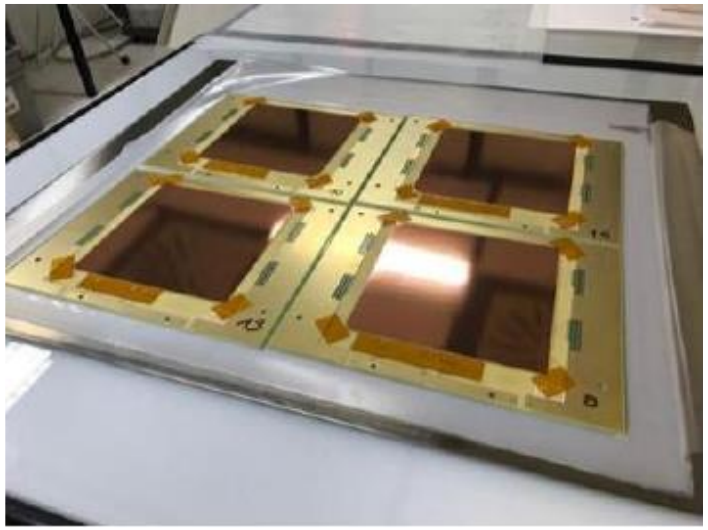

Production Tests @ ELTOS, large area detectors (w/CMS):

- 1.2x0.5m^2 with strip r/o
- 1.9x1.2m^2 with strip r/o - (**w/PCB splicing**)

Test on going: # 8 chamber of 30x30 cm2 @ ELTOS

The etching of the kapton still done by Rui @ CERN

High rate layouts: relevant parameters

	SG1	SG2	SG2++	DRL	SRL
Grid-pitch (mm)	6	12	12	6	100
Dead zone (mm)	2	1.2	0.6	0	0
Geometric acceptance (%)	66	90	95	100	100
Conductive line width (mm)	0.3	0.3	0.1	-	-
DOCA	0.85	0.45	0.25	7	5.5
Ω_{eff} (MΩ)	134	209	200	270	1947
DLC resistivity (MΩ/□)	70	65	64	54	70

$\Omega \simeq \frac{\rho}{2} \times (pitch/2 + DOCA)/w$ → average resistance "seen" by a uniform particle flow irradiating the basic cell of the detector.
Ω summarizes the electrical and geometrical features of each current evacuation scheme.

Rate capability @ 90% vs $<\Omega_{eff}>$

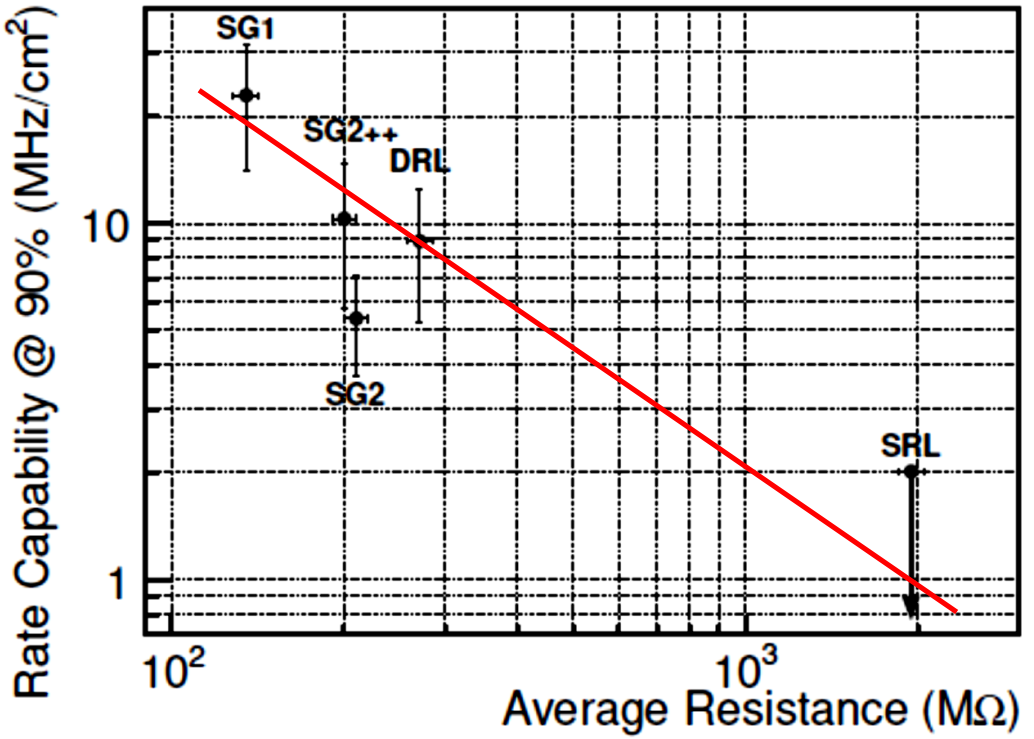

Rate capability at G/G_0 = 90% vs $<\Omega_{eff}>$: a gain drop of 10 % is largely acceptable since does not affect the detection efficiency (*as shown on slide #17*).

For the SRL, since the irradiation was not uniform, the measurement reported in this plot must be considered as an upper limit of its actual RC-90%.

Cluster Size

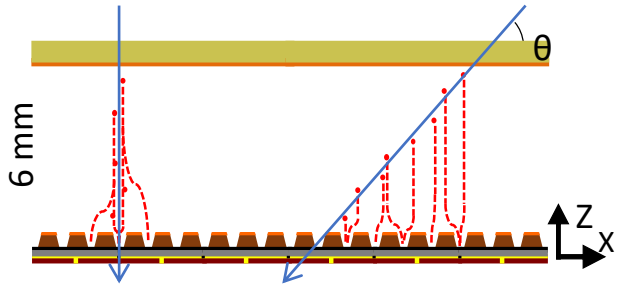

Ar/CO2/CF4=45/14/40

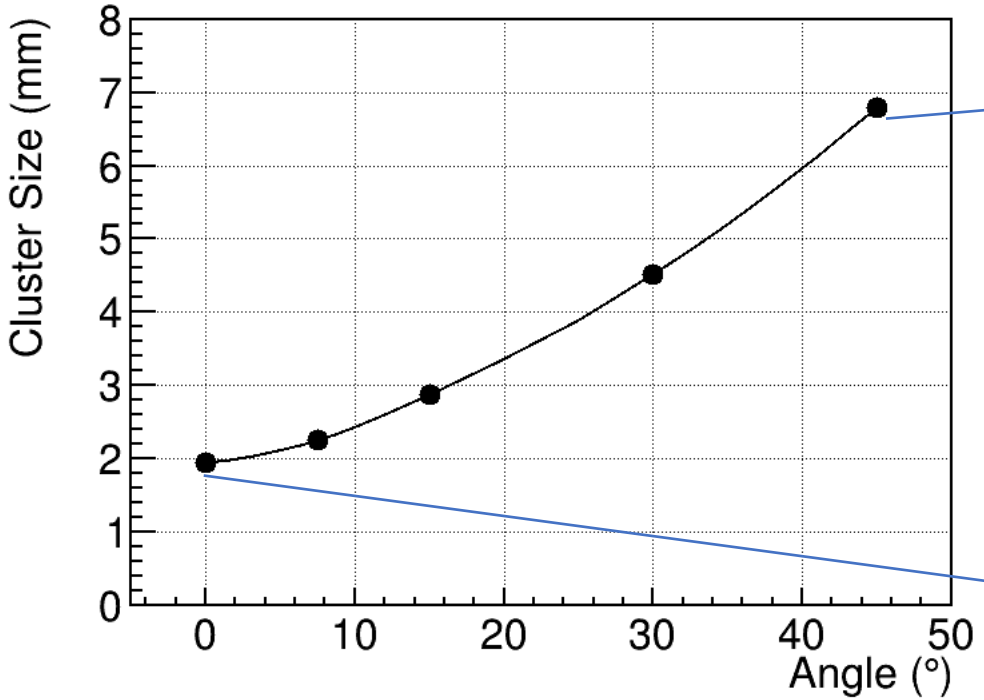

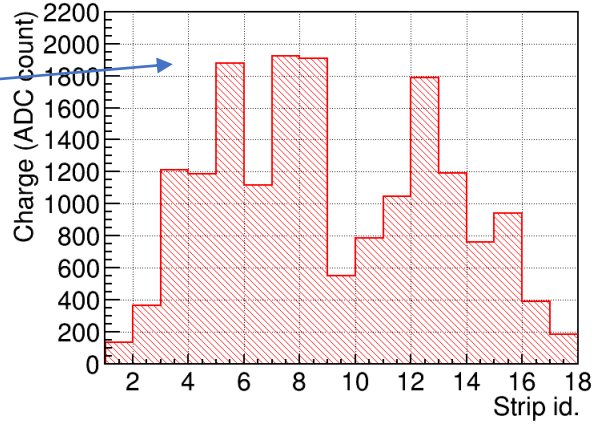

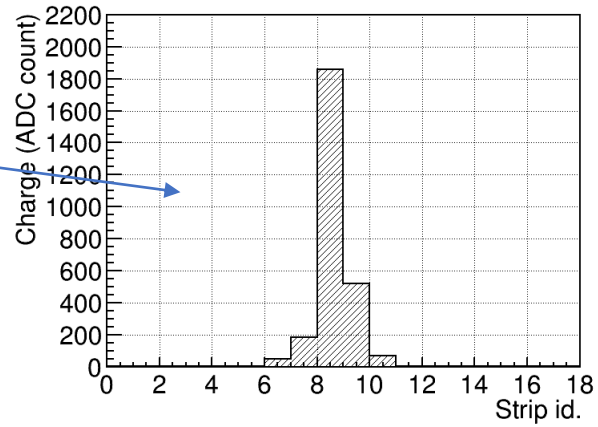

H4 Beam Area (RD51)

Muon beam momentum: 150 GeV/c

μ-RWELL with 400 μm pitch strips and readout by APV25

Drift gap 6 mm

Efficiency profile – SG1

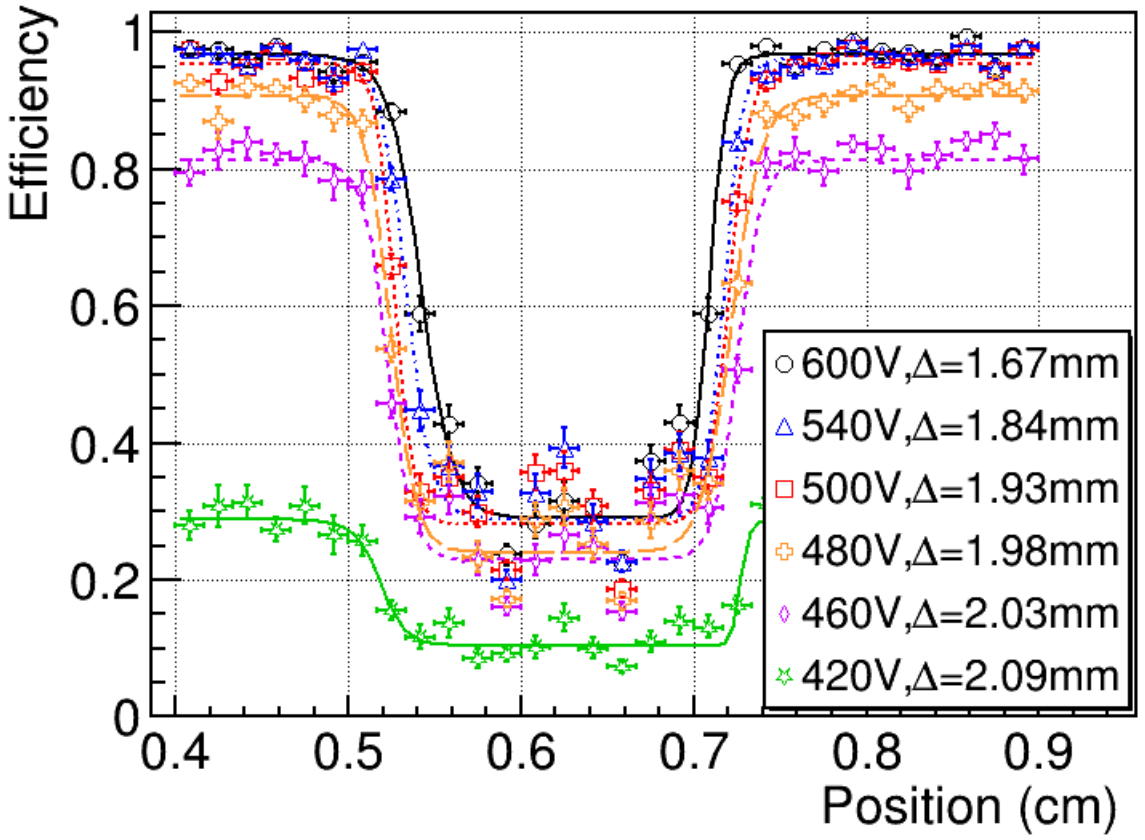

Space resolution *vs* DLC resistivity

With the charge centroid analysis (for orthogonal tracks) the track position is determined as a weighted average of fired strips.

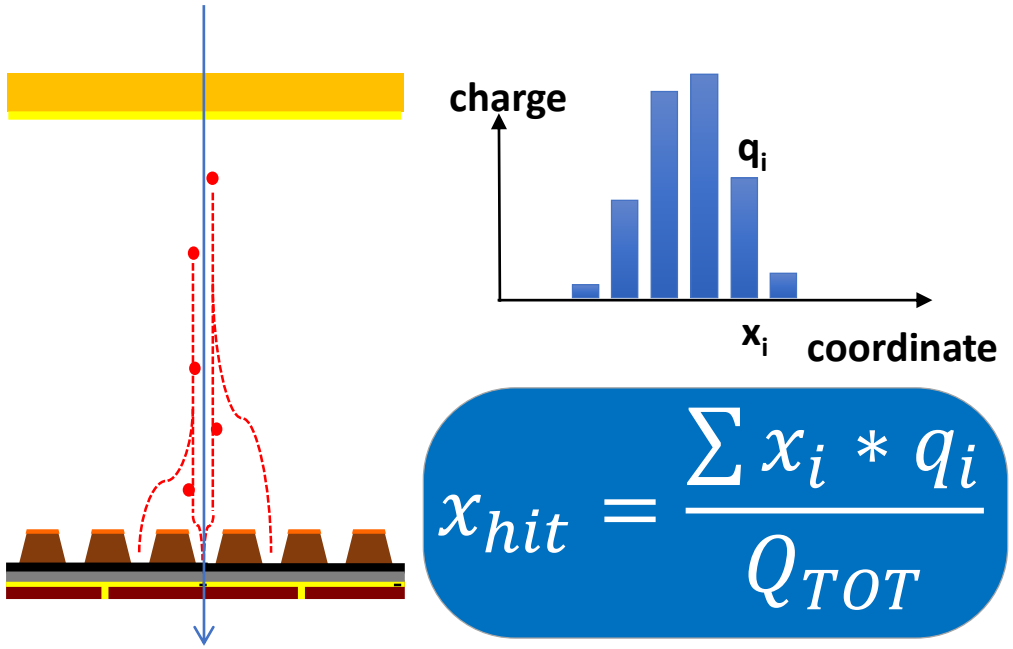

$$x_{hit} = \frac{\sum x_i * q_i}{Q_{TOT}}$$

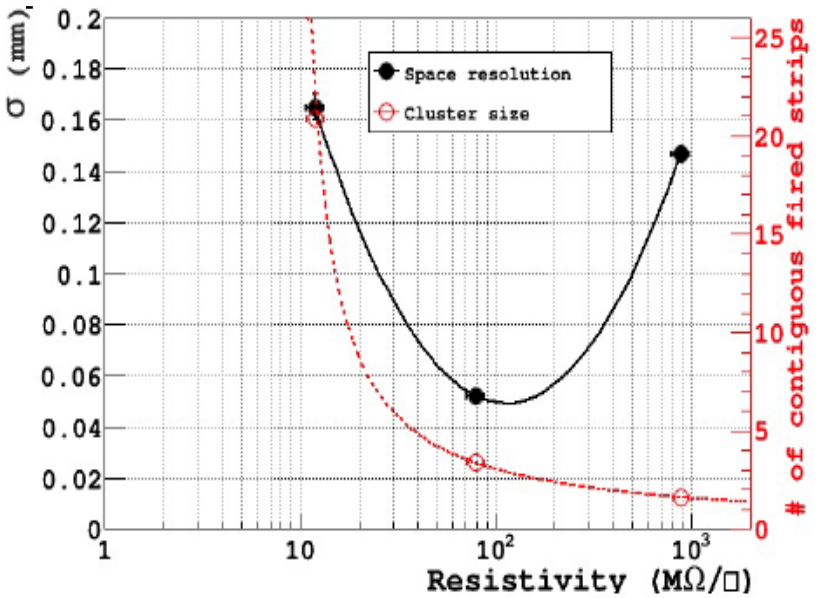

The space resolution exhibits a minimum around 100 MΩ/□:

- at low resistivity the charge spread increases and then σ is worsening
- at high resistivity the charge spread is too small (Cluster-size → 1 fired strip) then the Charge Centroid method becomes no more effective (σ → pitch/√12)

Ageing studies (on going)

GIF++ - Full area & Flux = 200 kHz/cm2

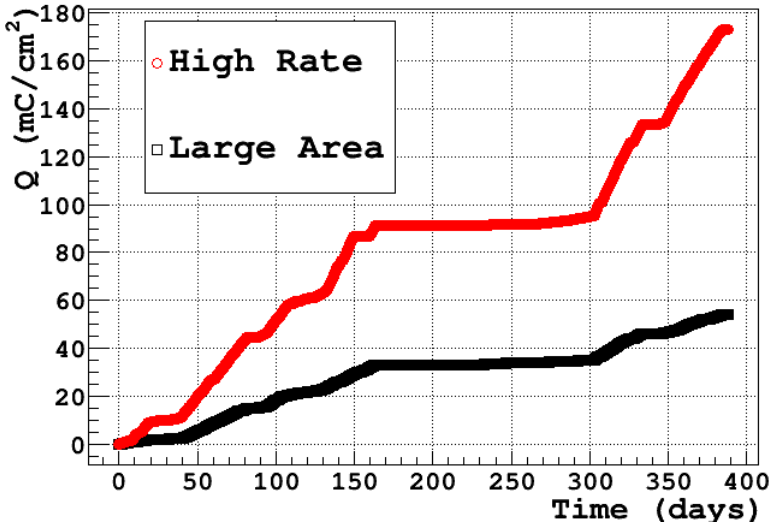

GOAL:
Integrate a charge up to 6 C/cm2

TB PSI – beam spot 9 cm2 – Flux= 10 MHz/cm2

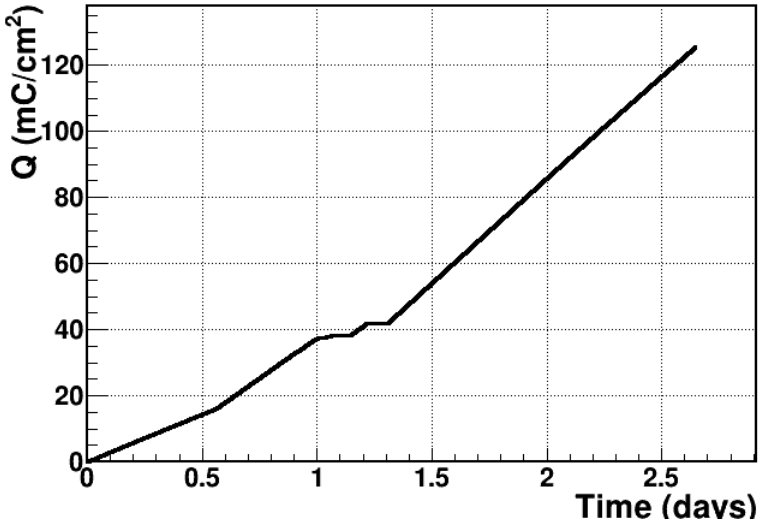

X-Ray gun- spot 50 cm2 Flux(rx) = 700 kHz/cm2

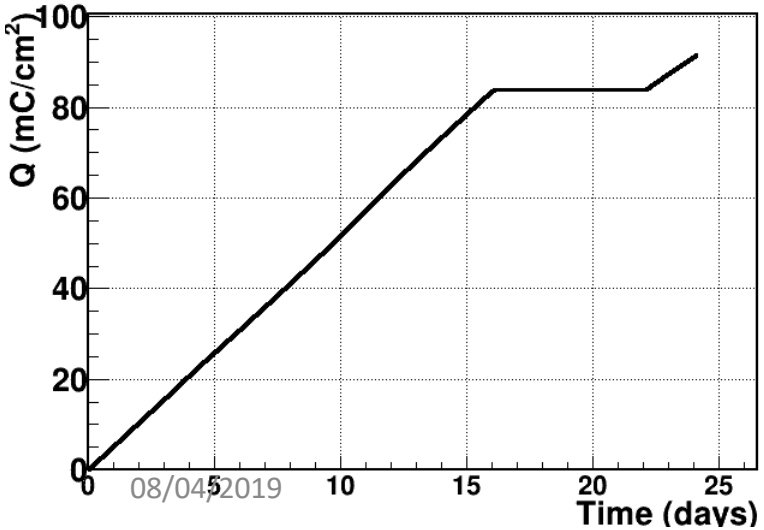

Slice test of μ-RWELLs during RUN3 in the Muon APPARATUS to be discussed

The LHCb Muon Apparatus

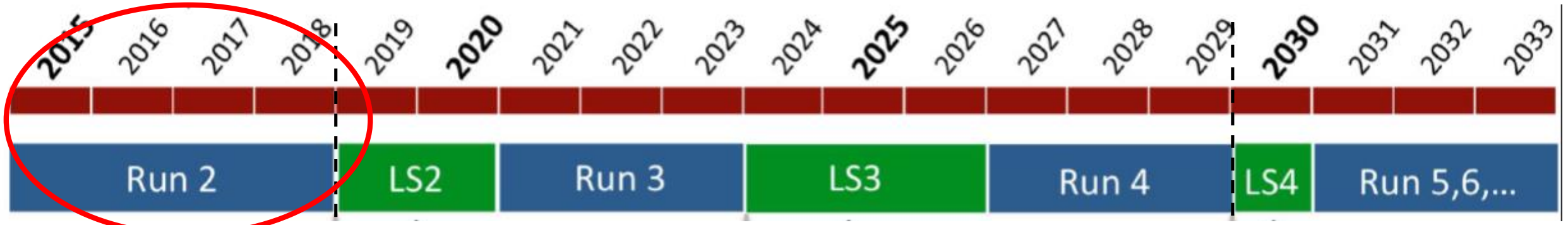

The Muon system has performed well in Run1 & Run2 @ 1-4x10^{32} (8 fb^{-1} collected)
→ tracking inefficiency due to dead time at level of 1 % in Run1 and 2 % in Run2

The consequences of the increase of the luminosity are

- large **increase of dead time inducing inefficiency** (in most region of the detector the reconstructed hits are obtained by crossing large area X & Y strips)
- **increase** of the rate of **ghost hits** from accidental crossing of X-Y channels
- **increase of the pion misidentification**

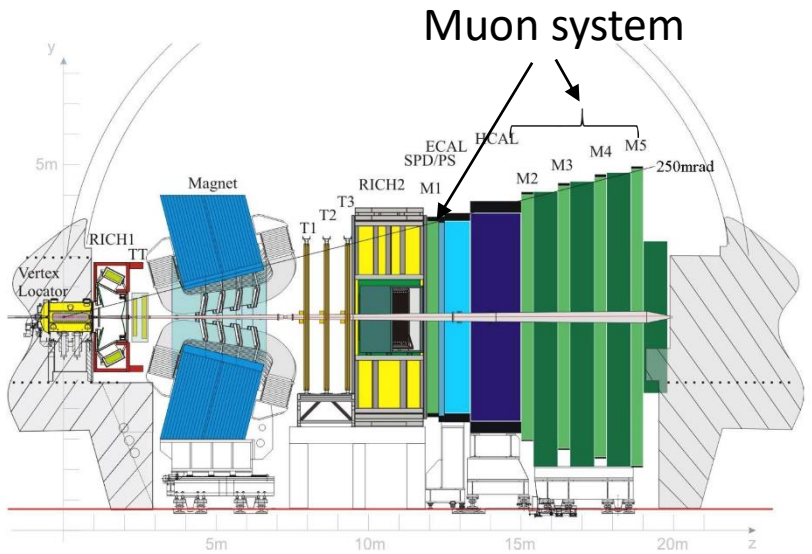

Current LHCb detector

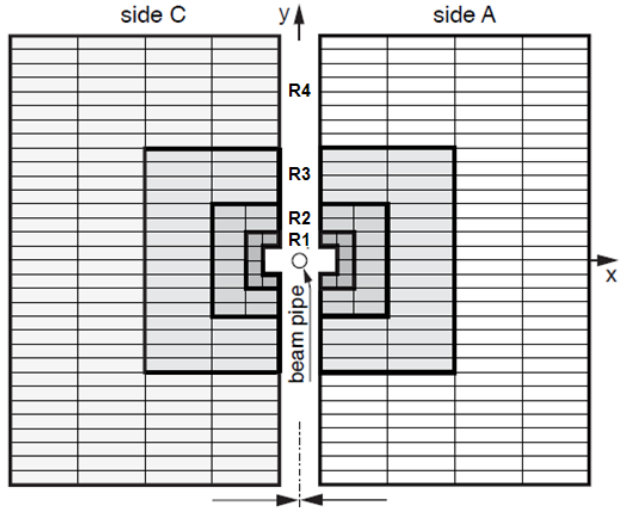

Muon system:
5 stations x 4 regions

The LHCb Muon Apparatus

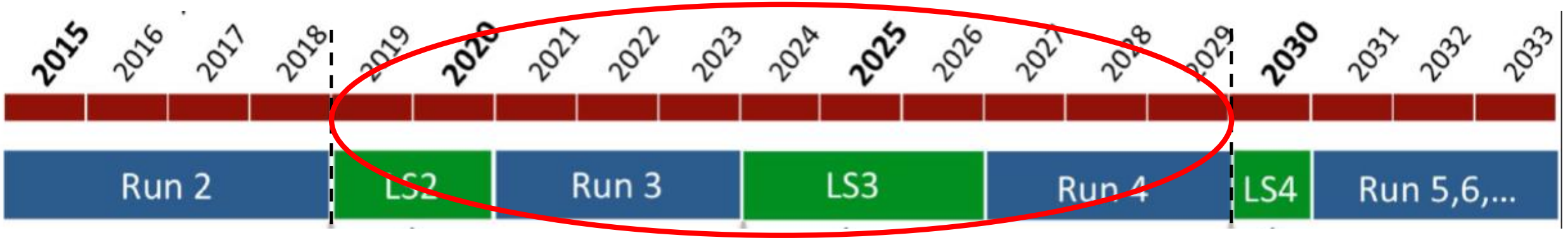

For **Run3 & Run4 @ 2x10^{33}** (foreseen to collect 50 fb^{-1}):

- **Improving the beam pipe shielding**
- **Increasing the granularity** of the most irradiated chambers

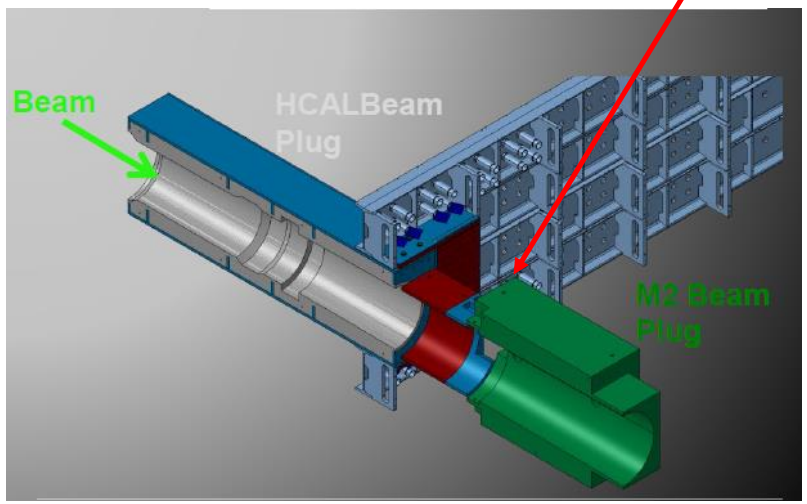

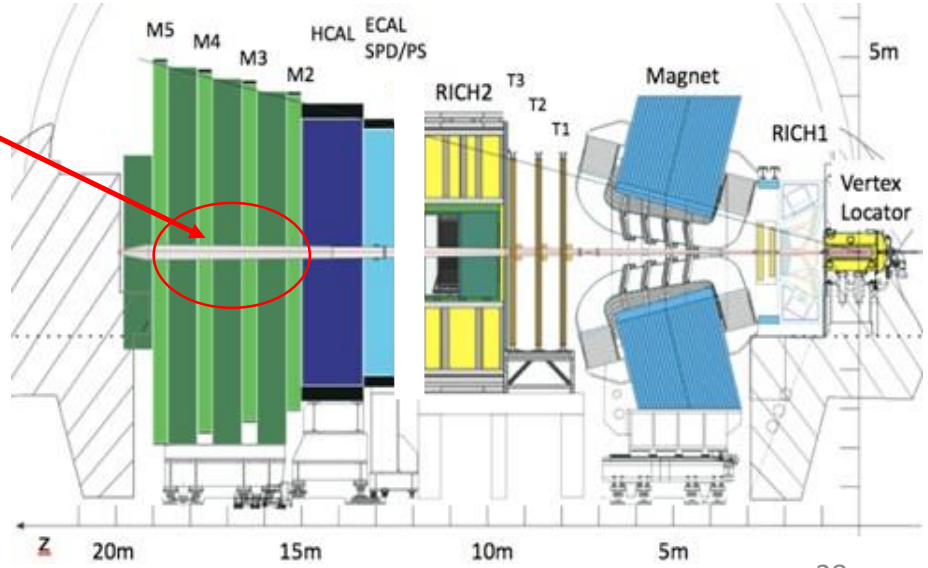

LHCb-INT-2017-019
LHCb-INT-2018-009

Muon Scenario

	A	B	C	D	E	F	G	H	I	J	K	L	M	N	O	P	Q	R	S	T
1		#cmb/region	cmb X (cm)	cmb Y (cm)	cmb Area cm	pad0 X (cm)	scale fact X	**pad X (cm)**	pad0 Y (cm)	scale fact Y	**pad Y (cm)**	pad Area (cm2)	max rate (kHz/cm2	**rate/pad (kHz)**	**C (pF)**	Nch/gap	Nch/2gap	Nch/region	ASIC/cha	ASIC/reg
2	M2R1	12	30	25	750	0,63	1,00	**0,63**	3,1	5,00	**0,62**	0,39	3300	1288	13,82724	1920	3840	46080	30	**360**
3	M2R2	24	60	25	1500	1,25	2,00	**0,63**	6,3	5	**1,26**	0,79	300	236	27,8775	1904	3808	91392	29,75	**714**
4	M2R3	48	120	25	3000	2,5	2,00	**1,25**	12,5	5	**2,5**	3,13	35	109	110,625	960	1920	92160	15	**720**
5	M2R4	192	120	25	3000	5	1,00	5,00	25	1	25	125,00	20	2500	4425	24	48	9216	0,375	72
6	M3R1	12	32	27	864	0,67	1,00	**0,67**	3,4	5,00	**0,68**	0,46	1900	865	16,12824	1896	3792	45504	29,625	**355,5**
7	M3R2	24	65	27	1755	1,35	2,00	**0,68**	6,8	5	**1,36**	0,92	220	201	32,4972	1911	3822	91728	29,859375	**716,625**
8	M3R3	48	130	27	3510	2,7	2,00	**1,35**	13,5	5	**2,7**	3,65	19	69	129,033	962	1924	92352	15,03125	**721,5**
9	M3R4	192	130	27	3510	5,4	1,00	5,40	27	1	27	145,80	5	729	5161,32	24	48	9216	0,375	72
10	M4R1	12	35	29	1015	2,9	4,00	**0,73**	3,6	5,00	**0,72**	0,52	650	339	18,4788	1944	3888	46656	30,375	**364,5**
11	M4R2	24	70	29	2030	5,8	8,00	**0,73**	7,3	5	**1,46**	1,06	85	89	37,4709	1917	3834	92016	29,953125	**718,875**
12	M4R3	48	139	29	4031	11,6	7,00	**1,66**	14,5	5	**2,9**	4,81	9	43	170,1222857	838	1676	80448	13,09375	**628,5**
13	M4R4	192	139	29	4031	23,1	1,00	23,10	29	1,00	29	669,90	3	2009	23714,46	6	12	2304	0,09375	18
14	M5R1	12	37	31	1147	3,1	4,00	**0,78**	3,9	5,00	**0,78**	0,60	550	332	21,3993	1897	3794	45528	29,640625	**355,6875**
15	M5R2	24	74	31	2294	6,2	8,00	**0,78**	7,7	5	**1,54**	1,19	55	65	42,2499	1922	3844	92256	30,03125	**720,75**
16	M5R3	48	149	31	4619	12,4	7,00	**1,77**	15,5	5	**3,1**	5,49	7	38	194,3965714	841	1682	80736	13,140625	**630,75**
17	M5R4	192	149	31	4619	24,8	1,00	24,80	30,9	1,00	30,9	766,32	4	3065	27127,728	6	12	2304	0,09375	18

The choice on the granularity would be a compromise among:

- Max rate per channel: 1 MHz/ch to keep occupancy under control (1MHz == 2.5% occupancy???)
- Capacitance/ch < 100 pF
- ASIC density/gap: depends on power consumption, to be investigated

Gaps not in OR (as in the table):

☺ **Low pad capacitance < 100 pF**

☹ **High ASIC density on detector & high number of FEE channels**

Gaps in OR:

☺ **For R1&R2 the FEE channels are divided by a factor of 2**

☺ **For R3 due to the constraint of pad capacitance, the number of pads doubles, the FEE channels remain the same wrt gaps not in OR**

LHCb UPGRADE

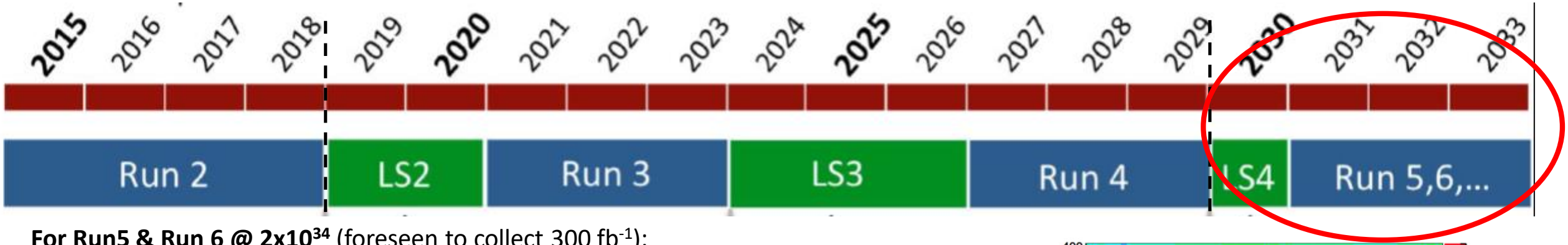

For Run5 & Run 6 @ 2x10^{34} (foreseen to collect 300 fb^{-1}):

- ❑ **Replace the HCAL** with **with a new Wall**
  - iron core 1.7 m in front of R1, R2, R3 (5.6 Λ → 10.1 Λ)
  - iron/concr./iron (30/110/30 cm) in the middle plane, to get a similar thickness as HCAL (6.2 Λ)
  - concrete 1.7 m top/bottom (4 Λ)

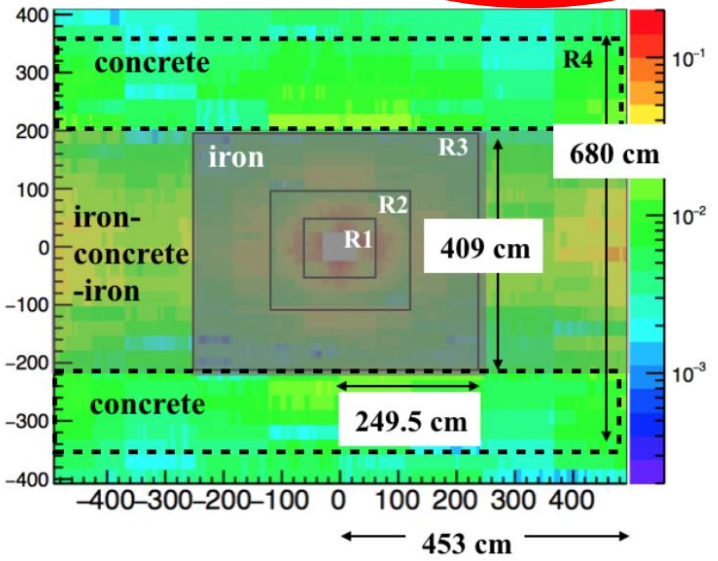

- ❑ **Install new detectors on the Muon apparatus**

	kHz/cm^2		kHz/cm^2		kHz/cm^2		kHz/cm^2
M2R1	3300	M3R1	1900	M4R1	650	M5R1	550
M2R2	300	M3R2	220	M4R2	85	M5R2	55
M2R3	35	M3R3	19	M4R3	9	M5R3	7
M2R4	20	M3R4	5	M4R4	3	M5R4	4